Photoproduction of Single Neutral Pions from Hydrogen at Energies 0.6 to 1.2 BeV*

R. DIEBOLD†
California Institute of Technology, Pasadena, California
(Received 21 January 1963)

Measurements of the differential cross section for the process $\gamma+p \rightarrow \pi^0+p$ have been made at three pion center-of-mass angles: 60°, 90°, and 120°. Values were obtained at intervals of 0.05 BeV (incident laboratory photon energy, k) from approximately 0.6 to 1.2 BeV. Most of the data were obtained by detecting only the recoil protons with a large, wedge-shaped, single-focusing magnetic spectrometer and associated equipment. For $\theta'_{\pi^0}=60°$ and $k\leq 0.94$ BeV the π^0 decays were also required, the decay photons being detected by a lead glass total absorption counter. Although the experimental resolution was considerably narrower than that of most of the previous experiments, its averaging effect was still appreciable in certain regions. Using a six-parameter fit, the data at each angle were unfolded in an effort to eliminate the effects of resolution and to obtain the true cross sections as a function of energy. The results compare reasonably well with those of previous experiments once differences in resolutions and systematic errors are taken into account. The results did not agree with the predictions of a simple resonance model with the resonance quantum numbers suggested by Peierls. The positions and widths of the two cross-section peaks in this energy region are quite similar to those observed in $\pi^- p$ scattering.

I. INTRODUCTION

DURING the past several years the photoproduction of neutral pions at energies above the first resonance has been the subject of numerous experiments. The cross section has been measured in this high-energy region by several methods: detection of the recoil proton only, using a counter telescope[1–3] or magnetic spectrometer[4]; detection of the π^0 decay only[5]; and detection of both the recoil proton and the π^0 decay.[6–8] In spite of the vast amount of effort spent on these experiments, no clear picture of either the angular distributions or the variation of the cross section with energy was obtained. This is perhaps not only the result of the broad resolutions used in many of the experiments, but also the difficulty encountered in making corrections to the results for detection efficiency and contamination from other processes.

The experiment discussed in this article was performed in an effort to obtain a better idea of the variation of cross section with energy. In particular, it was hoped that good values for the positions and widths of the peaks in the total cross section at $W\approx 1.5$ and 1.7 BeV (total c.m. energy) could be obtained and a comparison made with the $\pi^- p$ scattering peaks. For this purpose the cross section was measured at $\theta'_{\pi^0}=60°$, 90°, and 120° (prime refers to the c.m. system) for $0.6\lesssim k\lesssim 1.2$ BeV at intervals of 0.05 BeV (k is the incident laboratory photon energy). Where possible, the experimental conditions were arranged so as to minimize the systematic errors to which some of the previous experiments were prone. Most of the data were obtained by detecting only the recoil proton with a magnetic spectrometer and associated equipment. For $\theta_\pi'=60°$ and $k\leq 0.94$ BeV the π^0 decay was also required.

The 60° results were previously reported in preliminary form[9]; they are described and analyzed in greater detail in this article. The values have shifted slightly reflecting a more careful analysis of the corrections.

II. EXPERIMENTAL METHOD

A. Beam and Target

The photon beam used to study the reaction was obtained from the Caltech synchrotron which typically accelerated 3×10^9 electrons per pulse (once per sec). The electrons were allowed to strike a tantalum radiator over a period of 40 msec, thus producing a bremsstrahlung beam. This beam was collimated into a rectangular shape which was 4 cm broad and 5 cm high at the position of the target. The photon energy spectrum and the geometric distribution of the beam intensity were measured by J. Boyden and R. L. Walker. They found the spectrum to be intermediate between that expected for a thin radiator and for the 0.2 radiation length radiator used. The angular distribution of the beam was such that at one BeV the full width at half-intensity was 4 cm at the position of the target (10 m from the radiator). The beam intensity was monitored by an ion chamber, the charge output of which was integrated to give the total amount of beam during each run. The ion chamber

* Work supported in part by the U. S. Atomic Energy Commission.
† Present address: CERN, Geneva, Switzerland.
[1] P. C. Stein and K. C. Rogers, Phys. Rev. **110**, 1209 (1958).
[2] R. M. Worlock, Phys. Rev. **117**, 537 (1960).
[3] K. Berkelman and J. A. Waggoner, Phys. Rev. **117**, 1364 (1960).
[4] J. I. Vette, Phys. Rev. **111**, 622 (1958).
[5] R. M. Talman, C. R. Clinesmith, R. Gomez, and A. V. Tollestrup, Phys. Rev. Letters **9**, 177 (1962).
[6] J. W. DeWire, H. E. Jackson, and R. Littauer, Phys. Rev. **110**, 1208 (1958); H. E. Jackson, J. W. DeWire, and R. M. Littauer, Phys. Rev. **119**, 1381 (1960).
[7] G. Cortellessa and A. Reale, Nuovo Cimento **18**, 1265 (1960); G. Cortellessa, A. Reale, and P. Salvadori, Estratto dai Rendiconti dell'Istituto Superiore di Sanità **23**, 1177 (1960).
[8] M. Deutsch, C. Mencuccini, R. Querzoli, G. Salvini, G. V. Silvestrini, and R. Stiening, in *Proceedings of the Aix-en-Provence Conference* (Centre d'Etudes Nucleaires de Saclay, Seine et Oise, 1961), p. 9.
[9] R. Diebold, R. Gomez, R. Talman, and R. L. Walker, Phys. Rev. Letters **7**, 323 (1961).

was frequently calibrated by R. Gomez using a Wilson quantometer.[10]

The target was a cylindrical Mylar cup filled with liquid hydrogen. The axis of the cup was in the vertical direction and the diameter was 7.5 cm; it was surrounded by a series of heat shields which were cooled by liquid hydrogen and nitrogen reservoirs. The liquid hydrogen in the cup was kept at a pressure of 15 psi, giving a density of 0.0707 g/cm^3 and an effective length of 0.50 g/cm^2 of hydrogen in the beam path. A lead slit was placed near the target to prevent protons produced in the heat shields from reaching the spectrometer.

B. Proton Detection

A wedge-shaped, uniform field, single focusing magnetic spectrometer was used to momentum analyze the protons. Particles with momentum ≤ 0.62 BeV/c can be analyzed with the configuration shown in Fig. 1; by changing the geometry of the system one can analyze particles with momentum ≤ 1.17 BeV/c. Both configurations were used in this experiment. Counter $A1$ limits the spectrometer solid angle in the vertical direction. The "fan" counters limit the acceptance in the horizontal direction; they also eliminate particles scattering from the magnet pole faces. Counter $C2$ limits the momentum acceptance of the system to $\Delta p/p \approx 4\%$. Protons were distinguished from other particles (mainly positive pions) by a time-of-flight measurement between counters $A1$ and $C2$ and by pulse-height requirements in scintillation counters $C1$, $C2$, and $C3$. For the points with high proton momenta, a Lucite Čerenkov counter was placed between counters $C1$ and $C2$ to aid in the separation of protons from pions. Measurements of the proton absorption indicated that, depending on the momentum, 5 to 12% of the protons were absorbed by the system.

Fixing two parameters (such as the proton lab angle and momentum) in a two-body process fixes all other parameters including the photon energy. The energy resolution of the experiment, thus, depended on how precisely the proton parameters were determined by the spectrometer. It also depended to a lesser extent on the finite size of the beam-target interaction volume and, for the low-momentum points, on multiple scattering and energy loss in the target. The full width at half-maximum, Δk, of the resolution function was approximately proportional to k for a particular center-of-mass angle, the average values of $\Delta k/k$ being 0.11, 0.07, and 0.05 for $\theta'_{\pi^0}=60°$, 90°, and 120°, respectively.

C. π^0 Decay Photon Detection

For the $\theta'_{\pi^0}=60°$ and $k\leq 0.94$ BeV points, the π^0 decay photons were detected in two different ways. The first required a pulse from the large lead glass total absorption counter (see Fig. 1) in coincidence with a proton, while the second required a pulse from both the lead glass counter and the scintillation counter $1A$ in coincidence with a proton. The lead glass counter was 30 cm high, 36 cm wide, and 36 cm deep; counter $1A$ was only 16 cm high and 20 cm wide. A 2.3-radiation-length lead converter was placed in front of counter $1A$ so that the π^0 decay γ rays could produce electron showers and be counted by counter $1A$. No veto counter was used to eliminate charged particles, nor was any aperture built to limit the acceptance of the lead glass counter (edge effects were small, since most of the π^0 decays resulted in a photon passing through the central region of the counter).

The geometric efficiency of the lead glass counter ranged from 90 to 100% for the various points at which the counter was used, while that of counter $1A$ ranged from 50 to 90% (these efficiencies were calculated with a Monte Carlo program by R. Talman). The efficiency of the lead converter was calculated to be 78%. Taking into account the geometric and conversion efficiencies for detecting the π^0 decay, the two counting rates agreed

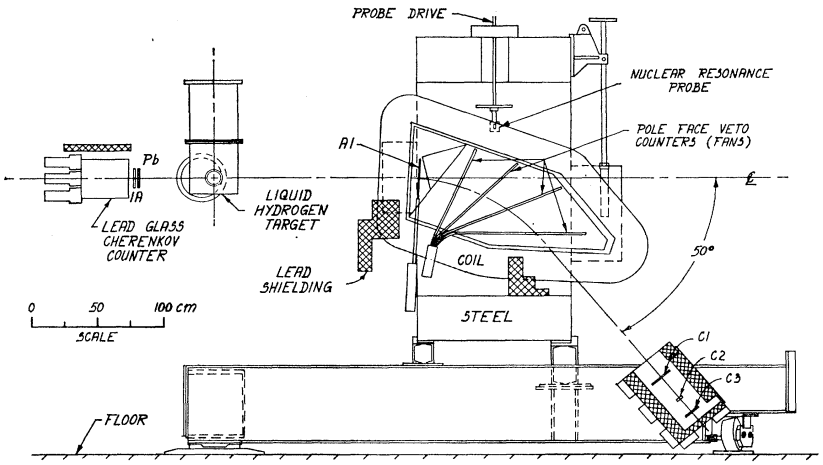

FIG. 1. Experimental apparatus. The magnetic spectrometer is shown in the position used to analysis particles with momenta ≤ 0.62 BeV/c. For the higher momentum points the geometry of the system was altered and a lucite Čerenkov counter was placed between $C1$ and $C2$. For convenience the figure shows both sets of equipment at right angles to the beam. Actually the spectrometer was approximately 56° and the decay photon equipment 38° from the beam direction for the 60° points; for the 90° and 120° points the spectrometer was approximately 41° and 27°, respectively, from the beam direction.

[10] R. R. Wilson, Nucl. Instr. 1, 101 (1957).

with one another quite well. Because of its reduced efficiency counter 1A was not used in the cross-section determination.

D. Photon Energy Consistency Checks

Series of runs were made by fixing the spectrometer parameters and varying E_0, the bremsstrahlung end point energy. The position of the step in the counting rate due to single π^0 photoproduction from hydrogen served to test the consistency between (1) k determined by the spectrometer settings, (2) E_0 determined by integrating the magnetic field of the synchrotron, and (3) the gross shape of the photon spectrum near the end point energy. The runs also gave a rough check on the resolution widths.

For each spectrometer point so studied, a curve was calculated which was proportional to the expected counting rate. The data were then least-squares fit by adjusting the proportionality constant and by "sliding" the curve along the horizontal (energy) axis. One of these checks is shown in Fig. 2. To get a good fit it was necessary to "slide" the curve to the left by 0.012±0.003 BeV from the position expected to the position shown in the figure. Three other checks were also made; the average discrepancy was 0.007±0.003 BeV. The discrepancy can be accounted for by assuming any one of the following: the magnet was set to lower momentum or smaller angle than thought; the true value of E_0 was 0.8% higher than measured by the synchrotron magnetic field integrator; or the photon spectrum had a sharper cutoff near the end-point energy than was assumed. Since the source or sources of the discrepancy are not known, it was attributed equally to k and E_0 in the analysis (only the determination of the central photon energies of the points is sensitive to the source of the discrepancy).

III. DATA REDUCTION

A. Counting Rate Corrections

1. Empty Target Background

The largest correction to the recoil proton counting rate was the background from beam interactions in the 0.012-cm-thick Mylar walls of the cylinder containing the liquid hydrogen. This background was measured by taking runs with the cylinder emptied of all but an atmosphere of gaseous hydrogen at liquid-hydrogen temperature. Because this background came mainly from complex nuclei, it did not fluctuate rapidly with spectrometer setting; for this reason it was measured at only every second or third point, and the results interpolated to the other points.

The empty target correction to the counting rate at $\theta_\pi' = 60°$ was about 50% of the rate from hydrogen when detection of the π^0 decay was not required. Requiring the π^0 decay in coincidence with the recoil proton reduced this to 1 or 2%. At 90° and 120° the background was typically 15% of the hydrogen rate.

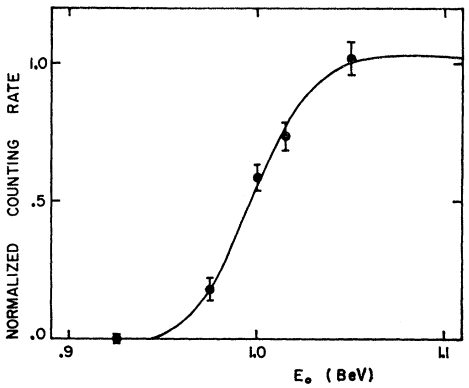

FIG. 2. Photon energy consistency check. The points were obtained by fixing the spectrometer momentum and angle to observe recoil protons produced in association with single neutral pions at $\theta'_{\pi^0} = 120°$ by a photon of approximately 1.0 BeV; E_0 is the bremsstrahlung end-point energy. The calculated response, shifted to the left by 0.012 BeV to give a best fit to the data, is also shown.

2. Below Threshold Background

Early in the experiment it was observed that the proton counting rates *from hydrogen* at $\theta_\pi' = 60°$ were approximately 15% higher than expected on a basis of the proton plus γ-ray coincidence rates. The difference in rates was found to be independent of E_0 to within statistics, even when E_0 was lowered to a value such that recoil protons from either π^0 production or Compton scattering were kinematically excluded from the spectrometer (the proton plus γ-ray coincidence rates from hydrogen went to zero at the low value of E_0). Thus, the excess protons do not appear to be direct recoils from the photoproduction of any particle. A mass spectrographic analysis of the hydrogen indicated that the effect was not the result of impurities in the hydrogen.

Detailed calculations were made to determine if the effect was a result of nuclear scattering processes which depend on the presence of hydrogen in the target (otherwise the empty target runs would cancel it out). The hydrogen dependence can come from two different types of processes: (1) The hydrogen can scatter protons and neutrons (the neutrons produce recoil protons); and (2) It can produce high-momentum protons which then scatter in the target or from the lead slit placed next to the target. The calculations could account for only about one quarter of the observed effect, however, and the main source of these protons thus remains a mystery.

For the 60° points at which the π^0 decay was detected the cross sections were obtained from the proton plus lead glass counter coincidence rates; since the below threshold background did not contribute to this counting rate, no correction was necessary for these points. Corrections for the background at the other points were made on the basis of runs taken with low values of E_0 at a few of the points. At 90° and 120° the effect was found to be only 2 or 3% of the π^0 counting rate.

3. Pion Pair Contamination

In order to reduce the contamination from the processes

$$\gamma+p\rightarrow\pi^0+\pi^0+p,$$
$$\gamma+p\rightarrow\pi^+\pi^-+p,$$

E_0 was generally set as low as possible consistent with not cutting sharply into the single π^0 production counting rate.

Extra runs were made with high values of E_0 at a few of the points in order to measure the strength of the pion pair processes. On the basis of these runs corrections were made to the data using the assumption that the energy dependence of the pion pair cross section is proportional to the phase space involved. The corrections were all found to be less than 1%.

The results of the high E_0 runs were used to obtain the sum of the differential cross sections for the two processes shown above. Chasan *et al.*[11] have measured the differential cross sections for photoproducing charged pion pairs in hydrogen (the second process). Comparing the two sets of data one obtains the result that neutral pion pairs are photoproduced in hydrogen only 0.2 ± 0.4 times as often as are the charged pion pairs.

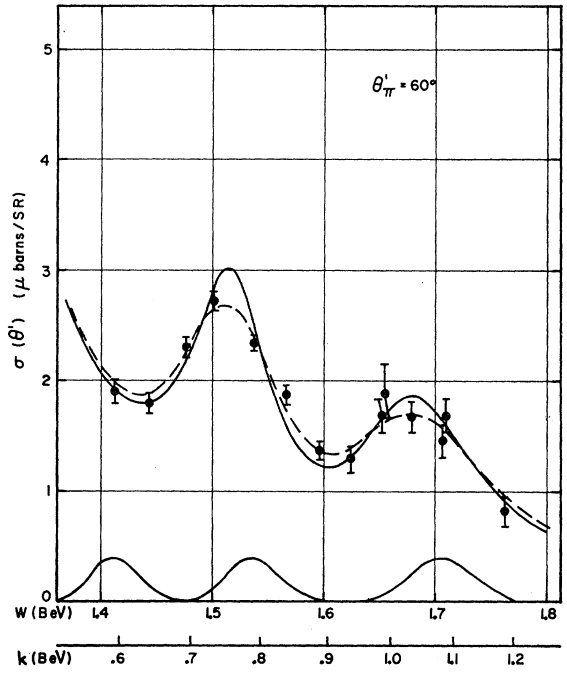

FIG. 3. The experimental 60° c.m. differential cross sections are shown as the points. The error flags reflect the random and rapidly varying uncertainties of the points; not shown is the 5% uncertainty in absolute normalization. The solid curve is the unfolded fit to the data at this angle; it is the result of a calculation made to eliminate the averaging effect of the experimental resolution. The dashed curve shows the effect of such averaging on the unfolded fit; it is this curve which should be compared with the points. Typical resolution functions are shown at the bottom of the figure. W is the total center-of-mass energy, while k is the laboratory energy of the incident photon.

[11] B. M. Chasan, G. Cocconi, V. T. Cocconi, R. M. Schectman, and D. H. White, Phys. Rev. **119**, 811 (1960).

4. Compton Scattering Contamination

Compton or elastic scattering of photons from protons is experimentally quite similar to single π^0 photoproduction; for this reason there was no simple way to experimentally obtain an estimate of its effect on this experiment. The existing experimental data above the first resonance are quite meager.[12,13] An attempt to calculate the cross section by assuming that only a few terms are important has been made by Berkelman, who found that at these energies there is a strong dependence on the π^0 lifetime.[14] In any case the Compton cross section appears to be only a few percent of the single π^0 cross section. Because of the uncertainty in the cross section for this contamination no attempt was made to correct for it, and the results of this experiment are very nearly just the sum of the Compton and single π^0 cross sections (the factors relating counting rates to cross sections for the two processes are nearly equal because of the similarity of the processes).

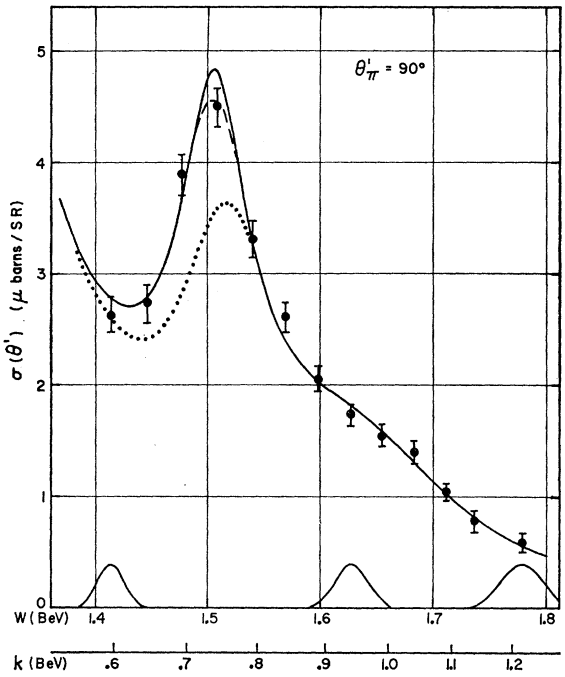

FIG. 4. Results for $\theta_\pi'=90°$. The dotted curve shows the 90° results of the fit described in Sec. IVC. The dotted and dashed curves are shown only in the region in which they differ appreciably from the unfolded fit.

[12] J. W. DeWire, M. Feldman, V. L. Highland, and R. Littauer, Phys. Rev. **124**, 909 (1961).

[13] G. Cortellessa, A. Reale, and P. Salvadori, Estratto dai Rendiconti dell'Istituto Superiore di Sanità **23**, 1188 (1960).

[14] K. Berkelman, Istituto Superiore di Sanità Report ISS 61/13 (1961) (unpublished).

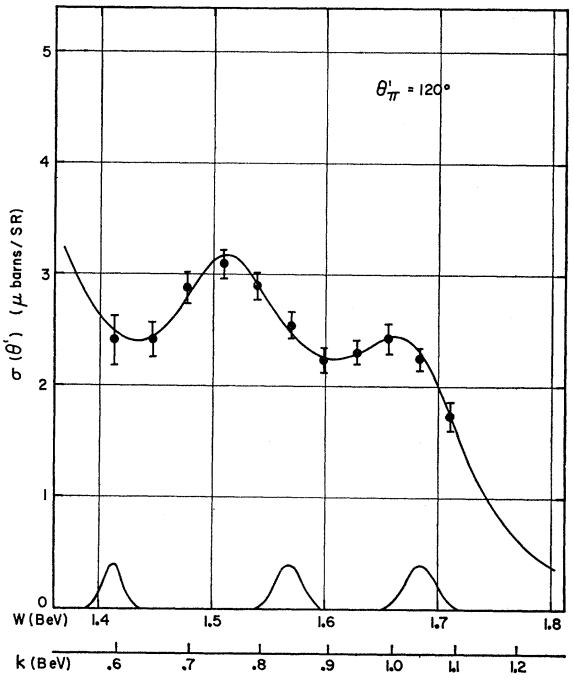

FIG. 5. Results for $\theta_\pi' = 120°$. The dashed curve is not shown since the narrow experimental resolution at this angle did not have an appreciable averaging effect.

B. Errors

Neither the counting-rate corrections nor various of the factors needed to convert the counting rates to cross sections are known precisely. The uncertainties in these quantities combine with counting statistics to give an uncertainty in the cross sections. These errors (considered as standard deviations) are conveniently grouped according to their variation with photon energy:

1. Constant or Slowly Varying Errors

a. Beam calibration: 4%.
b. Spectrometer acceptance, $\Delta\Omega\Delta p/p$: 3%.
c. Hydrogen in beam: 1%.

2. Random or Rapidly Varying Errors

a. Counting statistics: typically 6%.
b. Empty target background: typically 3%.
c. Below threshold background: 0.5 to 5%.
d. Pion pair contamination: ≈1%.
e. Proton absorption: 1%.

The errors of group 2 were combined to give the standard deviation of each of the experimental points; it is this uncertainty which is shown by the error flags on the points in Figs. 3–5.

TABLE I. Tabulation of the cross sections obtained experimentally at pion c.m. angle θ'_{π^0} and total c.m. energy W; also listed is the incident photon energy k. These results are also shown as the points in Figs. 3–5. As discussed in the text and demonstrated in the figures, these values need to be corrected for the averaging effect of the experimental resolution. The errors given are the standard deviations corresponding to the random and rapidly varying uncertainties of the measurements; not included is the 5% uncertainty in absolute normalization.

θ'_{π^0} (deg)	W (BeV)	k (BeV)	$\langle\sigma(\theta')\rangle_{av}$ (μb/sr)
60	1.412	0.594	1.90±0.11
60	1.442	0.639	1.79±0.09
60	1.476	0.692	2.30±0.08
60	1.501	0.732	2.73±0.09
60	1.537	0.790	2.33±0.06
60	1.566	0.837	1.87±0.09
60	1.596	0.888	1.37±0.08
60	1.624	0.936	1.29±0.12
60	1.652	0.985	1.68±0.15
60	1.654	0.989	1.88±0.28
60	1.679	1.033	1.67±0.14
60	1.706	1.082	1.45±0.15
60	1.709	1.088	1.68±0.16
60	1.762	1.185	0.82±0.13
90	1.413	0.595	2.63±0.16
90	1.445	0.644	2.73±0.18
90	1.477	0.694	3.89±0.19
90	1.508	0.743	4.50±0.18
90	1.539	0.793	3.31±0.17
90	1.568	0.841	2.61±0.14
90	1.598	0.891	2.06±0.11
90	1.627	0.942	1.73±0.10
90	1.654	0.989	1.55±0.10
90	1.682	1.039	1.40±0.10
90	1.710	1.089	1.05±0.07
90	1.736	1.137	0.79±0.08
90	1.779	1.217	0.60±0.08
120	1.413	0.595	2.40±0.22
120	1.446	0.645	2.41±0.16
120	1.477	0.694	2.87±0.15
120	1.509	0.744	3.09±0.13
120	1.539	0.793	2.89±0.12
120	1.569	0.843	2.54±0.12
120	1.598	0.892	2.23±0.11
120	1.627	0.942	2.30±0.11
120	1.655	0.991	2.42±0.14
120	1.683	1.041	2.24±0.10
120	1.710	1.090	1.73±0.13

IV. RESULTS AND DISCUSSION

A. Data and Unfolded Fits

The values of $\langle\sigma(\theta')\rangle_{av}$ obtained by the experiment are tabulated in Table I and are shown as the points in Figs. 3–5 (the cross section is averaged by the finite experimental resolution). As previously mentioned these results are actually the sum of the single π^0 production and Compton scattering cross sections, the latter presumably being only a few percent of the total.

Typical energy resolution functions are shown at the bottoms of the drawings. The 60° points have considerably wider resolution than do the other points because of unfavorable kinematic conditions; this wide resolution resulted in a considerable broadening of the peaks. An attempt was made to eliminate the effects of resolu-

tion by assuming that the cross sections at each of the three angles could be approximated by a general shape with six free parameters. At each angle these parameters were adjusted to give the best statistical fit to the data. The general shape which was used for this unfolding process was the superposition of three resonances and their interference terms.

The strength of the 3-3 resonance in this high-energy region was obtained from the formula of Gell-Mann and Watson which successfully fits the experimental data in the region of the resonance.[15] The shapes of the other two peaks were obtained from similar resonance formulas which at these high energies yield curves closely resembling simple Breit-Wigner curves. The six free parameters used for the fitting were the positions, widths, and strengths of these two peaks. The interference terms were obtained by assuming the peaks to be resonances with the quantum numbers suggested by Peierls.[16] Thus, the first resonance was assumed to be $P_{3/2}$ initiated by a magnetic dipole interaction; the peak near $W=1.5$ BeV (total c.m. energy) was taken to be a $D_{3/2}$ resonance initiated by an electric dipole interaction; and the peak near 1.7 BeV was assumed to be an $F_{5/2}$ resonance initiated by an electric quadrupole interaction. The signs of the amplitudes were chosen to give the polarization of the recoil proton in the direction observed experimentally.[17]

The fits were obtained by calculating the cross-section curve for a particular set of the six parameters and then averaging it in the same way as the experimental resolution averages it. The results were compared with the experimental results obtained for the angle being fit; the six parameters were then adjusted to give a better fit. This process was repeated many times; the best of the unfolded fits are shown as the solid lines in Figs. 3–5. The dashed curves show the effect of the experimental averaging in those regions where it was appreciable; it is these dashed curves which should be compared with the experimental data in such regions. The three fits were all statistically good.

The best values for the differential cross sections at the three angles are felt to be those obtained by these fits in spite of the fact that they do depend slightly on the particular form of the fitting functions used. Not only do these fits unfold the effects of resolution, but they also tend to smooth out the random statistical fluctuations.

B. Contour Map

Rather than show explicitly the angular distributions obtained at the 11 energies measured by this experiment, a different scheme has been used to display the angular distribution as a function of energy. Figure 6 shows lines of constant differential cross section as a function of the total center-of-mass energy and $\cos\theta'_\pi$. The positions of the contour lines in the region measured by this experiment were determined by the unfolded fits. The results of numerous other experiments were used to extend the map into other regions. The choice of which data to use and how to interpret it was somewhat arbitrary; the deciding factor was often an artistic one. A careful examination of the various possible systematic errors and the effects of wide resolution was not made for the other experiments; these effects were taken into account, however, but in a subjective manner.

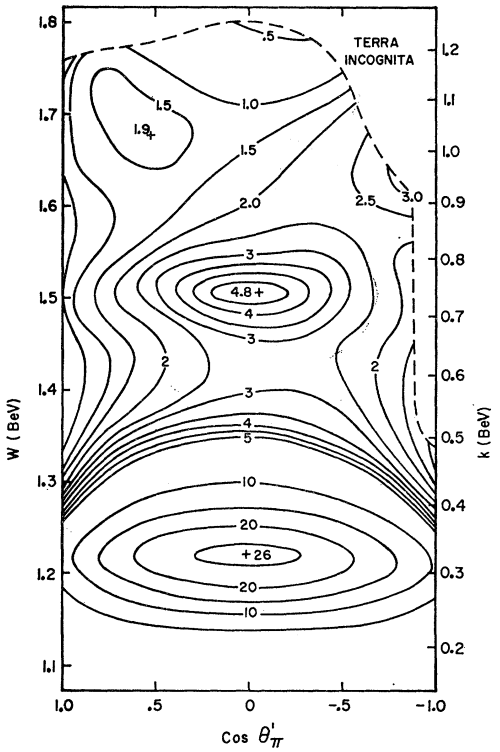

FIG. 6. Lines of constant differential cross section for $\gamma+p\rightarrow\pi^0+p$, as obtained in a subjective manner from various experiments, including the present one. The contour interval changes from 5 to 0.5 μb/sr in going from the first to second peak.

C. Resonance Model Fit to All the Data

An attempt was made to fit all the data of the experiment using the assumption that only the three resonant amplitudes used for the unfolding fits are important. The interference terms of these amplitudes were found to introduce an asymmetry between 60° and 120° which did not agree with the data. For this reason a small amount of electric dipole s wave (corresponding to 0.3 μb/sr if it were the only term) was introduced with a 0° phase shift. Although the s-wave interference effects helped the fit considerably, at energies above the third resonance the interference terms change sign

[15] M. Gell-Mann and K. M. Watson, Ann. Rev. Nucl. Sci. 4, 219 (1954).
[16] R. F. Peierls, Phys. Rev. 118, 325 (1960).
[17] J. O. Maloy, G. A. Salandin, A. Manfredini, V. Z. Peterson, J. I. Friedman, and H. Kendall, Phys. Rev. 122, 1338 (1961).

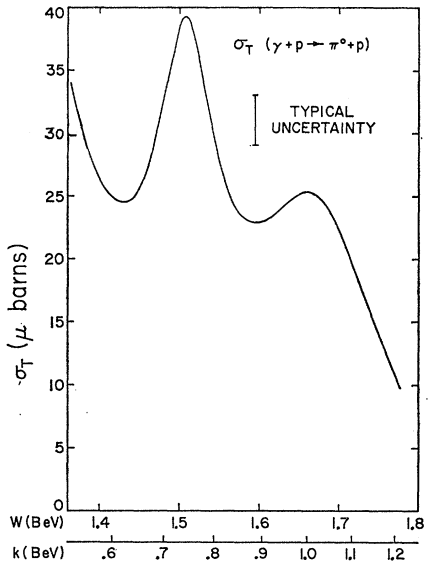

FIG. 7. The total π^0 photoproduction cross section as obtained from the quartics in $\cos\theta'$ passing through the results of this experiment and the 30° and 150° differential cross sections obtained from Fig. 6. The large uncertainty in $\sigma(150°)$ is the dominant contributor to the uncertainty in σ_T.

and the fit is still rather poor in this region. The fitting process was similar to that of the unfolded fit except that all the data were being fit with seven parameters (six parameters for the second and third resonances and one for the s-wave amplitude). The best fit was statistically quite poor: $\chi^2=150$ for only 33 degrees of freedom. Not only was the fit unable to give the right interference signs above the third resonance, but it was also unable to fit the large 90° cross section near $W=1.5$ BeV (see Fig. 4).

If one constrains the angular distribution to be positive at all angles and to pass through the values obtained by this experiment, then in the region near $W=1.5$ BeV fourth order or higher terms are needed in an expansion of the form $\sigma(\theta')=\sum_i a_i \cos^i\theta'$. Under the assumptions made as to the character of the resonances, fourth-order terms come only from the third resonance which is not strong in this region. It would, thus, appear that different or additional terms are important in this region, and that simple resonances with the quantum numbers of Peierls cannot adequately describe the phenomena.

D. Total Cross Section

Too few angles were measured by this experiment to yield reasonable angular distributions without further information since at least third- and fourth-order terms are important. To supplement the information obtained by this experiment, values of $\sigma(30°)$ and $\sigma(150°)$ were obtained from Fig. 6 at several energies. At each energy the quartic polynomial in $\cos\theta'$ passing through the five values of differential cross section was used to compute the total cross section; the results are shown in Fig. 7. The greatest uncertainty in this determination comes from the uncertainty in $\sigma(150°)$.

E. Comparison with Previous Experiments

The unfolded 90° results of this experiment are shown in Figs. 8 and 9 as the solid curves. The broken line curves of the same figures show the results expected, on the basis of the unfolded fit, from experiments with resolutions widths of $\Delta k/k=0.10$ and 0.20. The 90° results of the previous experiments are also shown in the figures; the resolutions of the previous Caltech and Cornell experiments[1–6] fall between 0.10 and 0.20 while those of the Frascati experiments are approximately 0.06[7] and 0.03.[8]

The results of Cortellessa and Reale[7] do not agree with those of the other experiments including this one. With this exception the results of the previous experiments, while in substantial agreement with this experiment, tend to be 5 to 10% higher at 90°. The 60° data of this experiment are in slightly better agreement with the earlier experiments than are the 90° data. At 120° the previous results are higher than those of this experiment by about 15%. While the 5 or 10% discrepancy at 90° can perhaps be explained on the basis of known systematic errors such as the uncertainty in beam calibration, the 15% at 120° cannot be so explained. Some of this 15% discrepancy is perhaps the result of errors in the large corrections which had to be made at this angle by some of the previous experiments for such effects as pion pair production and nuclear absorption.

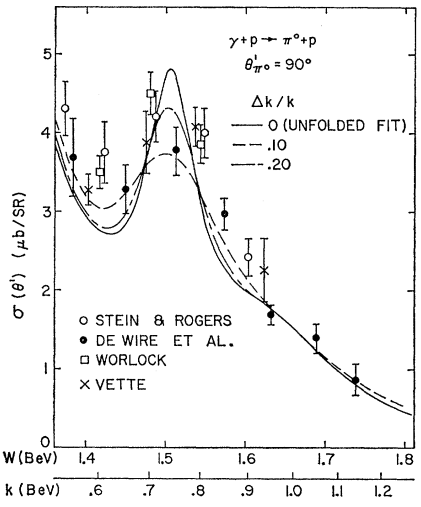

FIG. 8. Comparison of the 90° results of this experiment with those of previous Cornell and Caltech experiments (references 1, 6, 2, and 4). The solid curve shows the unfolded fit of this experiment; the broken line curves show the results expected, on the basis of the unfolded fit, from experiments with resolution widths of $\Delta k/k=0.10$ and 0.20 (Δk is the full width at half-maximum of the resolution function and k is the incident photon energy). The resolutions of the old Cornell and Caltech experiments lie between 0.10 and 0.20.

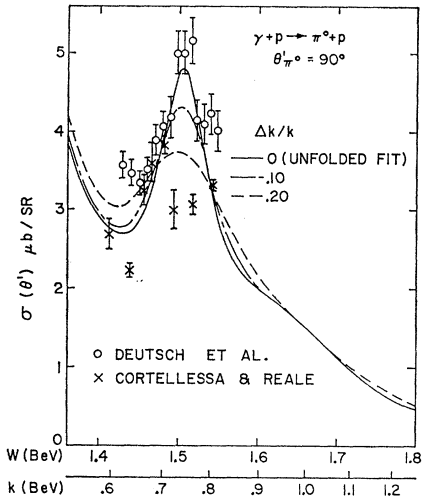

FIG. 9. Comparison of the 90° results of this experiment with those of the Frascati experiments. The resolution width of Deutsch *et al.* (reference 8) is typically $\Delta k/k=0.03$, while that for Cortellessa and Reale (reference 7) is typically 0.06.

F. Comparison with Other Reactions

It is interesting to compare the π-nucleon scattering and the π photoproduction cross sections. The most obvious characteristics to compare are the positions and widths of the peaks in the cross sections when plotted as a function of energy. It was hoped that the positions and widths of the single π^0 photoproduction peaks could be obtained from the total cross section since it is not affected by interference terms between simple multipole states. The quartic fit total cross section was not used, however, for this determination because it depended on the 30° and 150° cross sections which were measured by other experiments with large errors.

Table II shows the parameters obtained for the second and third peaks by an examination of the results of the three unfolded fits and the fit made to all the data. The errors reflect not only the statistical uncertainty of the experiment, but also the spread in the results obtained by the various fits. For completeness the first resonance parameters, as obtained by fitting the early experiments with the formula of Gell-Mann and Watson[15] are also shown. The parameters obtained from pi-nucleon scattering[18–21] are also listed in Table II. It is interesting to note that the parameters as determined by the two types of reactions agree with one another to within the uncertainties involved.

Since virtual particle exchange terms contain all angular momentum states and both isotopic spin states, they can interfere with simple multipole states even in the total cross section. If the peaks are really simple resonances as suggested by Peierls, then the principle effect of this interference in the total cross section is a shift in the energy of the peak position. Since the strengths of the different exchange terms vary with the reaction, the peaks for different reactions shift by varying amounts. The effect of the pion exchange term on the first and second resonance peaks has been studied by Wetherell.[22]

The differences between the positions of the π^0 and π^+ photoproduction peaks were calculated for both π^+ and ω exchange terms using the peak widths obtained by this experiment. For purposes of the calculation it was assumed that the peaks are resonances with Peierls' quantum numbers; the strength of the ω exchange term was obtained from the analysis of Talman *et al.*[5] The results of the calculation are shown in Table III; the effect of the ω exchange term is an order of magnitude less than that of the π^+ term and is in the opposite direction. The combined π^+ and ω shifts agree quite closely with the observed differences, which in the cases of the second and third peaks is perhaps surprising in the light of the results of the recent π-nucleon elastic

TABLE II. Summary of the resonance parameters obtained from both the π^0 photoproduction[a] and π-nucleon scattering[b] cross sections. The resonance energy, W_{res}, and the full width at half-maximum, ΔW, are both given in terms of the total center-of-mass energy and are in units of BeV. The term "resonance" is merely used for convenience; the second and third peaks are probably not simple resonances.[c]

Parameter	Reaction	Resonance 1st	Resonance 2nd	Resonance 3rd
W_{res}	$\gamma+p\rightarrow\pi^0+p$	1.238±0.005	1.517±0.006	1.692±0.008
W_{res}	$\pi^\pm+p\rightarrow\pi^\pm+p$	1.232±0.008	1.522±0.008	1.698±0.010
ΔW	$\gamma+p\rightarrow\pi^0+p$	0.112±0.010	0.090±0.014	0.130±0.018
ΔW	$\pi^\pm+p\rightarrow\pi^\pm+p$	0.106±0.006	0.087±0.012	0.100±0.012

[a] The first resonance parameters were obtained by fitting the data of the low-energy experiments with the formula of reference 15; the other π^0 production parameters were obtained by examining the results of the fits described in Secs. IVA and IVC.
[b] See references 18–21.
[c] See reference 21.

TABLE III. Relative positions of the cross section peaks. The term α is the difference between the positions of the π^0 and π^+ photoproduction peaks; β is the difference between the positions of the π^0 photoproduction peak and the π-nucleon scattering peak. Both α and β are in MeV.

Resonance	α calculated for π^+ exchange	α calculated for ω exchange	Observed α	β calculated for π^+ exchange	Observed β
1	15	−2	16± 6	5	6±10
2	21	−2	21± 8	14	−5±10
3	19	−1	17±14	13	−6±13

[18] S. J. Lindenbaum and L. C. L. Yuan, Phys. Rev. **100**, 306 (1955).
[19] J. C. Brisson, J. F. Detoeuf, P. Falk-Vairant, L. Van Rossum, and G. Vallandas, Nuovo Cimento **19**, 210 (1961).
[20] T. J. Devlin, B. C. Barish, W. N. Hess, V. Perez-Mendez, and J. Solomon, Phys. Rev. Letters **4**, 242 (1960).
[21] J. A. Helland, T. J. Devlin, D. E. Hagge, M. J. Longo, B. J. Moyer, and C. D. Wood, Phys. Rev. Letters **10**, 27 (1963).
[22] A. M. Wetherell, Phys. Rev. **115**, 1722 (1959).

scattering experiment at Berkeley[21] which indicate that neither of these peaks are simple resonances.

The Fermi-Watson theorem[23] relating the phase shifts of the S matrix to one another can be used in the calculation of the effect of particle exchange terms on the positions of the π^0 photoproduction peaks relative to the π-nucleon scattering peaks. The results of such a calculation are shown in Table III for the pion exchange terms; it was again assumed for the calculation that the peaks are resonances with Peierls' quantum numbers. Experimentally the π^0 photoproduction peaks are consistent with having the same positions as the scattering peaks, and except for the first resonance the positions are not consistent with the predictions based on the theorem. Since the theorem is valid only at low energies where multiple-pion production is negligible ($k \leq 0.4$ BeV), not much importance can be attached to this discrepancy.

ACKNOWLEDGMENTS

The author is deeply indebted to Professor Robert L. Walker for his suggestions, interest, and encouragement at all stages of the experiment. The 60° data were obtained in collaboration with Professor Walker, Dr. R. Gomez, and Dr. R. M. Talman.[9] F. Wolverton was of great assistance in obtaining the data at 90° and 120°. The author wishes to thank the various members of the Synchrotron Laboratory for their helpful comments and suggestions and for keeping the machine and peripheral equipment operating efficiently.

[23] K. M. Watson, Phys. Rev. **95**, 228 (1954).

PHYSICAL REVIEW VOLUME 130, NUMBER 5 1 JUNE 1963

Nonleptonic Hyperon Decays in the Pole Approximation and the Strong-Coupling Constants

JOGESH CHANDRA PATI
Institute for Advanced Study, Princeton, New Jersey
(Received 17 December 1962)

We have considered the nonleptonic hyperon decays $Y \to N+\pi$ in the baryon pole approximation, assuming the validity of the $|\Delta T| = \frac{1}{2}$ rule for the weak two-fermion ($Y \to N$) vertices. The ($\Sigma\Lambda$) relative parity is assumed to be even. We have tried to solve for the two strong-coupling constants g_Σ and g_Λ and the four weak-vertex parameters involved in ($\Sigma \to N$) and ($\Lambda \to n$) transitions from the known (experimental) hyperon-decay parameters. We find that there exist three solutions if $\Sigma^+ \to n+\pi^+$ proceeds via S wave (Case A): Solution (i)A, $g_\Lambda^2 \simeq 4g_\Sigma^2$, $g_\Sigma/g_N \simeq 0.6$; Solution (ii)A, $g_\Lambda^2 \simeq g_\Sigma^2$, $g_\Sigma/g_N \simeq -1.2$; and Solution (iii)A, $g_\Lambda^2 \simeq g_\Sigma^2/4$, $g_\Sigma/g_N \simeq 1.3$; and only one solution if $\Sigma^+ \to n+\pi^+$ proceeds via P wave (Case B): Solution B, $g_\Lambda^2 \simeq g_\Sigma^2$, $g_\Sigma/g_N \simeq 0.94$. These solutions are quite different from those given previously by Singh and Udgaonkar; the main reason for the difference is that they use a value of unity for the $|P/S|$ ratio in $\Lambda \to p+\pi^-$ decay, while we use a value of nearly 0.36 for the same ratio, as found experimentally. We apply all the four solutions to radiative $Y \to N+\gamma$ decays and point out experiments which could distinguish between these solutions. Given the results of a few experiments, one may be in a position to choose the most favored solution and predict the results of other experiments, thus, subjecting the model to a direct test.

I. INTRODUCTION

SEVERAL authors[1] have considered the nonleptonic hyperon decays in the pole approximation and Singh and Udgaonkar[2] have demonstrated that one could get an insight into the signs and magnitudes of the $\Sigma\Sigma\pi$ and $\Sigma\Lambda\pi$ coupling constants, as well as which one of the $\Sigma^\pm \to n+\pi^\pm$ decays proceeds via S wave and which one via P wave, from the hyperon-decay parameters, if one considers that only the Σ, Λ, and N pole terms dominate the decay amplitudes. In fact, they demonstrated that if one accepts the criterion for choosing between different possible solutions that all the strong pion-baryon coupling constants should be comparable with each other, then $\Sigma^+ \to n+\pi^+$ is predicted to proceed via S wave and that $g_\Sigma \approx -\frac{2}{3}g_N$ and $g_\Lambda^2 \approx g_\Sigma^2$. [This is in the framework of even ($\Sigma\Lambda$) parity.]

The present work is partly identical in spirit to that of SU. Its purpose, however, is:

(i) Firstly, to point out that one has to radically alter the conclusions reached by SU, if one uses the correct values for the experimental quantities, specially the (P/S) ratio in Λ decay,[3] to which the analysis is quite sensitive.

(ii) Secondly, to consider the radiative hyperon decays $Y \to N+\gamma$ also in the baryon-pole approximation and to apply the solutions for the weak vertex

[1] G. Feldman, P. T. Matthews, and A. Salam, Phys. Rev. **121**, 302 (1961); J. Nuyts, thesis, University Libre de Bruxelles, 1961 (unpublished); S. K. Bose and R. Marshak, Nuovo Cimento **23**, 556 (1962); A. Fujii, Phys. Letters **1**, 75 (1962).

[2] V. Singh and B. M. Udgaonkar, Phys. Rev. **126**, 2248 (1962). This is referred to in this paper as SU.

[3] Singh and Udgaonkar (reference 2) have used the value unity for the $|(P/S)|$ ratio in Λ decay. The present value is: $|P/S|_\Lambda = 0.36_{-0.06}^{+0.05}$ (see reference 21).